ACS Sustainable Chemistry & Engineering

pubs.acs.org/journal/ascecg

Research Article

Environmental Sustainability of Mixed Cation Perovskite Materials in Photovoltaics Manufacturing

Sherif A. Khalifa, Sabrina Spatari, Aaron T. Fafarman, and Jason B. Baxter*

Cite This: *ACS Sustainable Chem. Eng.* 2020, 8, 16537−16548

Read Online

ACCESS | Metrics & More | Article Recommendations | Supporting Information

ABSTRACT: Efficiencies of lead halide perovskite photovoltaics have increased to 25%, putting them on track for commercialization within the next 1−3 years. Devices exhibiting the best combination of high efficiency and long operational lifetimes have used mixed cation perovskite absorber layers such as cesium/methylammonium/formamidinium lead iodide ($Cs_xMA_yFA_{1-x-y}PbI_3$). However, the associated environmental burdens of the supply chains of perovskite precursors should also be considered when selecting compositions for commercialization. Prior literature based on laboratory-scale data reported a particularly high environmental burden for FA and warned against using these highest-performing film compositions. Here, we report a comprehensive study of the environmental impacts of common precursor salts used to form mixed cation perovskite films, using a life cycle assessment approach. We have used updated data sources, process scale-up concepts, and sensitivity analysis to build commercial-scale life cycle inventory models for perovskite precursors that can inform industrial manufacturing choices with more transparent and robust environmental analysis. Our results indicate that the process-based climate change, cumulative energy demand, and human toxicity impacts of CsI, MAI, and FAI are similar to each other and lead to iodide (PbI_2) salts on a molar basis. The current cesium supply appears sufficient for near-future perovskite deployment. Additionally, the impacts of the perovskite precursors are ∼1000-fold smaller than those of glass when considering amounts needed per module area. Therefore, selection of perovskite composition can be based on PV efficiency and operational stability, without additional constraints of environmental impact.

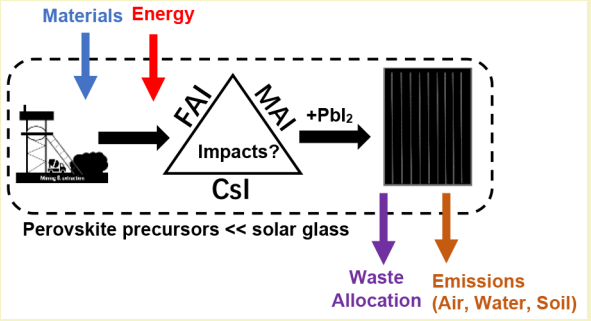

KEYWORDS: *Lead halide perovskite photovoltaics, Life Cycle Assessment, Supply chain sustainability, Material availability, Sustainable design, Thin film solar cells*

Downloaded via DREXEL UNIV on December 17, 2020 at 00:09:25 (UTC).
See https://pubs.acs.org/sharingguidelines for options on how to legitimately share published articles.

INTRODUCTION

Solar photovoltaic (PV) technologies are one of the fastest growing renewable energy sources and can provide clean electricity and mitigate climate change. PV met 2.5% of global electricity demand in 2019, and installed capacity of PV is expected to increase 10-fold in the next 30 years.[1,2] Crystalline silicon (c-Si) technologies currently provide ∼95% of the global PV market, with the balance from thin film technologies such as cadmium telluride. As energy demand continues to grow, further cost reductions and performance improvements are needed to scale up the sustainable electric power supply.

Emerging lead halide perovskite (LHP) materials show enormous promise as highly efficient, low-cost thin film PV absorber materials. The perovskite crystal structure has the chemical formula ABX_3, where A denotes a large cation, B is typically lead (Pb), and X is a halide (primarily iodide, I). The most studied cations include organic methylammonium (MA, $CH_3NH_3^+$) and formamidinium (FA, $CH(NH_2)_2^+$) and inorganic cesium (Cs) and rubidium (Rb). Efficiencies of single junction LHP solar cells rose from 3.8% in 2009 to 25.2% by late 2018, which is in line with the best current PV technologies.[3−5] Combined with rapid advances in scalable manufacturing and in operational stability, LHP PV are poised for commercialization in the next few years.[6−8] Perovskite thin films can enter the market as part of single-junction devices, perovskite-perovskite tandems,[9−11] or perovskite-silicon tandems.[12,13]

The chemical composition of the A-site cation of the perovskite strongly influences both power conversion efficiency and film stability.[14−17] In addition to requiring high efficiency, PV modules need to last at least 25−30 years in the field; degradation of the perovskite film has been one of the main challenges for commercializing LHP devices. Perovskite solar cells fabricated with long-studied MA-based formulations suffer from intrinsic instability even when the device is encapsu-

Received: August 2, 2020
Revised: October 7, 2020
Published: October 27, 2020

© 2020 American Chemical Society

https://dx.doi.org/10.1021/acssuschemeng.0c05619
ACS Sustainable Chem. Eng. 2020, 8, 16537−16548

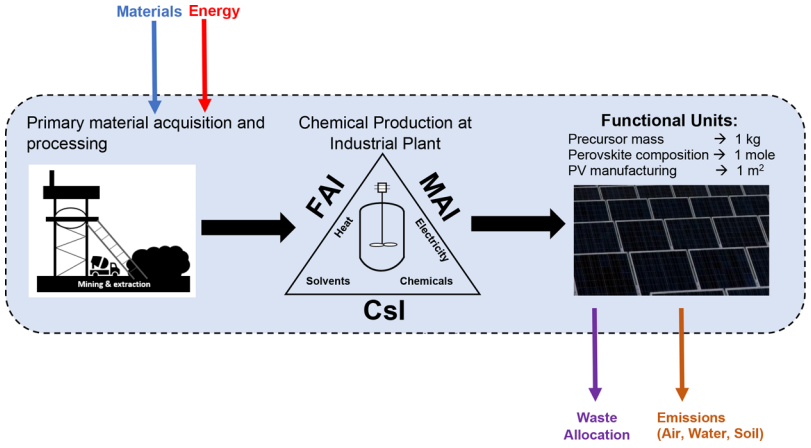

Figure 1. Cradle-to-gate life cycle flow diagram for production of perovskite cationic precursor materials in LHP PV systems. (Photo by Steve Wilcox, NREL 15539).

lated.[18,19] Alloying of the A-site cation, and to a lesser extent the X-site anion, has resulted in the best combinations of high efficiency and long operational lifetime. $MA_{0.05}FA_{0.95}PbI_3$ has shown record efficiency of 25.4% for all organic A-site cations.[20] Alloying with inorganic Cs can dramatically improve the thermal and structural stability of the perovskite phase. Saliba et al. showed that the triple-cation formulation $Cs_{0.10}MA_{0.15}FA_{0.75}Pb(I_{0.83}Br_{0.17})_3$ has a stabilized efficiency of 21.1%, with power output retained for 250 h in an aging test under operating conditions.[21] Many groups have eliminated MA altogether. $Cs_{0.25}FA_{0.75}PbI_3$ achieved 19.1% efficiency while maintaining full performance after 150 h at 85 °C in air.[22] The same formulation was also used in a perovskite−perovskite tandem device with 23.1% efficiency.[23] Turren-Cruz et al. reported promising results with $Cs_{0.15}FA_{0.85}PbI_3$ and $Cs_{0.10}FA_{0.90}PbI_3$ which achieved high and stable efficiencies of 17.4% and 19.23%, respectively.[24]

To date, research has rightfully emphasized maximizing power conversion efficiency and operational stability, but the environmental impact should also be considered.[25,26] A few previous life cycle assessment (LCA) studies evaluated the impacts of mixed perovskite formulations in complete candidate LHP PV device architectures[27−29] or in the absorber layer alone.[30] Toxicity related to lead has been of significant concern. Our recent study indicated that the direct lead emissions and toxicity potential per kWh would be significantly lower for LHP PVs than for representative US grid electricity mixes under reasonable commercialization scenarios.[31] Nonetheless, detailed risk assessments and appropriate industrial hygiene practices should be implemented before commercialization. Beyond lead, some of the LCA studies found that other layers could have higher impacts than the perovskite absorber layer, although the studied device stacks are necessarily speculative since commercial products do not yet exist. In some cases, the layers found to have highest impact (e.g., Spiro-OMeTAD hole transport layer or gold back contact) are likely unscalable.

Focusing on the perovskite layer along with relevant sensitivity analysis on module manufacturing hotspots can provide insightful sustainability feedback until the research community reaches consensus on commercially viable device architectures. Perovskite films can be deposited in manufacturing lines using solution-based or vapor-based thin film coating processes, the former involving an additional step of dissolving the precursor salts in an appropriate solvent.[32] In either case, the fundamental chemical reaction takes the form $AX + BX_2 \rightarrow ABX_3$. Assuming high materials utilization efficiency in each process, both solution and vapor coating should employ similar amounts of precursor salts in their operation. Depositing mixed perovskite films would first require the industrial synthesis of AX and BX_2 precursor salts through either organic synthesis or mining and purification of inorganics. Inorganic minerals used as cations, cesium and occasionally rubidium, are listed in the top 35 minerals of critical supply in the U.S.[33]

In a recent effort to compare dependence of environmental impacts on perovskite composition, Alberola Borras et al. reported that films containing FA have significantly higher life cycle greenhouse gas (GHG) emissions in comparison to the canonical $MAPbI_3$.[30] This difference arose from a combination of different impacts calculated for FAI, MAI, and CsI precursors and the use of a chlorobenzene antisolvent step, but the relative importance of these two were not clearly distinguished. Their study warned against deployment of FA-containing formulations, raising potential concerns about the environmental sustainability of mixed cation LHP devices. Their life cycle inventory (LCI) inputs were based on laboratory-scale literature data and assumptions. However, the material and energy flows of small-scale production can be irrelevant to industrial manufacturing, which may involve different processes and equipment and are typically subject to greater design emphasis on efficiency. A more detailed analysis is needed on prospective upscaled production processes to accurately identify environmental impact-intensive hotspots.

Our objective is to investigate the life cycle environmental performance and resource requirements of scalable cationic precursor salts for LHP PVs, examining selected life cycle impact assessment (LCIA) metrics and critical element supply constraints, including sensitive inputs that lead to variability in environmental performance measures. We modeled a prospective production process for each cationic precursor (MAI, FAI, and CsI) for the ternary A-site composition space, while also noting a few specific A-site formulations that appear promising for commercialization. We also compared impacts of A-site cationic precursors to those of lead iodide (PbI_2) precursor and other module components (e.g., glass and PET substrates). This work aims to improve construction of the life cycle inventory through scale-up process design projections that may reduce uncertainty in sustainability evaluation,

https://dx.doi.org/10.1021/acssuschemeng.0c05619
ACS Sustainable Chem. Eng. 2020, 8, 16537−16548

thereby supporting commercial decision-making related to perovskite PV technology.

METHODS

This study applies an attributional LCA framework following the International Organization for Standardization (ISO140/44)[34,35] to investigate the environmental impacts of prospective upscaled perovskite cationic precursors used in manufacturing LHP PV systems. We selected a cradle-to-gate system boundary that includes the life cycle stages from mining and extraction of raw materials to the entry gate of a perovskite module manufacturing facility (Figure 1). We followed process design guidelines to calculate mass and energy balances along with estimating process fugitive emissions to construct an LCI model for each of the process steps in the system boundary. We also calculated supply requirements of critical cesium to meet solar PV electricity generation requirements by LHP PVs over the next 30 years in U.S.[36]

Goal and Scope. We defined three functional units (FU) for reporting our impact assessment results. A FU of 1 kg of precursor is relevant for chemical plant operations. A FU of 1 mol is useful for researchers because chemical composition is reported on a molar basis. Finally, a FU of 1 m^2 of solar module defines the amount of precursor needed to manufacture 1 m^2 of perovskite thin film, which is relevant for comparing impacts with those of other module components.

The primary impact metrics studied here are climate change, cumulative energy demand (CED), and human toxicity (HT), calculated by ReCiPe v1.13.[37] We used the 100-year global warming potential (GWP) to quantify greenhouse gas (GHG) emissions that induce climate change impact, reported in kg CO_2 equivalents (eq). CED quantifies the direct and indirect energy consumption throughout the life cycle of a defined functional unit, reported in megajoules (MJ).[38] HT quantifies the human toxicity in units of kg of 1,4-dichlorobenzene (DCB) eq. We also use the USEtox model to distinguish between direct impacts on human health and terrestrial ecotoxicity of the A-site cationic formulations.[39,40] We could not use the USEtox model to evaluate the toxicity of lead halide salts because the model characterization factors for heavy metals have significant uncertainty.[41] The USEtox model reports the midpoint characterization factors for three impact categories: human toxicity- cancer, human toxicity- noncancer, and terrestrial ecotoxicity, factoring in environmental fate and exposure. The characterization factors for human toxicity are expressed in comparative toxic units (CTU_h), equivalent to human disease cases per unit of emitted chemical substance. Terrestrial ecotoxicity characterization factors are also expressed in CTU_e, estimating a potentially affected fraction of species per unit of emitted compound.

We kept transportation and infrastructure steps outside the studied system boundary due to the large uncertainty about the location of deployment. We assumed that their effects will be similar among all precursors and contribute relatively little impact compared to other process steps. Whenever possible, inventoried processes were kept to U.S. geography.

We used the LCI of scaled-up PbI_2 salt production previously reported by Gong et al.[42] to carry out a process-based impact comparison to A-site cation precursors (see Table S17 in Supporting Information (SI)). Nonetheless, we believe that a robust fate and exposure (i.e., ecotoxicological) risk assessment is still needed to complement LCA results for toxicity evaluation of lead usage in perovskite solar cells. We did not consider the impacts of lead(II) bromide ($PbBr_2$) precursor production because it has many possible synthesis routes, and we could not determine which one would be commercially feasible. However, $PbBr_2$ can be synthesized using the same PbI_2 process route involving the reaction of a potassium halide and lead nitrate.[43,44] In that case, the production processes for halide salts are reasonably similar except the usage of the respective iodine or bromine in upstream potassium halide production.[45] Iodine and bromine production processes have similar environmental impacts on a mass basis, where differences are not statistically significant, across all ReCiPe impact categories in ecoinvent database libraries. This makes our compiled LCI of PbI_2 production also suitable for modeling $PbBr_2$ production after carrying out a necessary correction for molecular weight.

Life Cycle Inventory (LCI) model development. We used Reaxys database libraries to identify high yield, industry-relevant process synthesis routes for each of the perovskite precursors. Then, we applied process design guidelines for prospective/ex-ante LCI models to sketch unit operations.[46−51] We used stoichiometry, thermodynamics, heat transfer, and chemical process modeling by ASPEN PLUS[52] to calculate the material and energy balances for unit operations. Scale-up methods by Piccino et al. were used for heated liquid-phase batch reactions for specialty chemicals to provide conservative estimations for upscaled material and energy inputs to LCI models. Where appropriate for a specific production process (i.e., triethyl orthoformate), ASPEN PLUS was used to estimate the energy consumption (e.g., cooling duty for subzero operating conditions) along with consulting theoretical approaches in scale-up literature. The LCA software tools SimaPro 9.1,[53] ecoinvent version 3.6,[54] and USLCI[55] database libraries were used to inventory the rest of the LCI inputs and run impact assessment.

A default electricity value of 0.33 kWh/kg of precursor salt was inventoried to account for plant-wide electricity consumption for pumping synthesis solutions as suggested by Hischier et al.[56] Fugitive emissions to air, water, and soil were estimated based on the phase and boiling points of the input materials.[57,58] The waste allocation decisions were made on a process-specific basis according to U.S. Environmental Protection Agency (EPA) waste handling guidelines and were reported in LCIs.[59,60] We also list the process selections made in SimaPro for transparency and reproducibility (see SI).

Production Capacity and Assumptions. We calculated the precursor salt demand, representing the system reference flow, to supply a PV manufacturing line of 100 MW of peak power (MWp) capacity (eq S1) as a reasonable near-future target. We assumed 100% precursor attribution in the perovskite A-site formulation as an upper limit estimation for MAI and FAI. We calculated CsI demand for 100% Cs and for $Cs_{0.15}FA_{0.85}$. We assumed a module efficiency of 17% for all calculations, which is an expected target of commercial single-junction perovskite modules to compete with existing PV technologies such as c-Si (16%−22%) and CdTe (17%)[61,62]

We also assumed a film thickness of 1 μm. Efficient lab-scale perovskite cells are made with 200−300 nm films. However, industrial-scale film coating processes might use thicker films to achieve better reproducibility and durability. Precursor demand for film thicknesses in the range of 300−1000 nm are reported in SI (see Table S3).

RESULTS AND DISCUSSION

Material Intensity of Perovskite Precursors. A material demand of 6.5 t (tonnes), 6.6 tonnes, and 10.6 tonnes for MAI, FAI, CsI are needed per GWp of PV modules, respectively, for films with pure A-site compositions. One GWp would supply ∼1% of the 2020 global PV market. The material required would decrease slightly with increasing PV efficiency (∼0.3 tonnes per 1% absolute) and would decrease proportionally with smaller film thickness. These relatively small scales (less than ∼500 tonnes/year) can most efficiently be produced by batch processing in an on-demand production facility commonly used in the specialty chemicals industry in a once-a-year fashion,[63] or more frequently if shelf life requires it.

The rental of on-demand manufacturing sites provides common chemical plant industrial equipment while avoiding the capital and environmental costs of building a new plant. Another advantage for batch processing is the high adaptability of unit operations to a wide variety of feeds and products as relevant for LHP precursor salts. If the LHP PV installation capacity increases, multiple on-demand production batches per

https://dx.doi.org/10.1021/acssuschemeng.0c05619
ACS Sustainable Chem. Eng. 2020, 8, 16537−16548

Table 1. Life Cycle Impact Results for Climate Change, CED, and HT Categories for Three Functional Units Defined as 1 kg, 1 mol, and 1 m^2 of Module for Each of the Cationic Precursor Salts for LHP Solar Cells

Precursor salt	MAI			FAI			CsI		
Functional Unit (FU)	1 kg	1 mol	1 m^2	1 kg	1 mol	1 m^2	1 kg	1 mol	1 m^2
Climate change[ab] (kg CO_2 eq)	38.1	6.06	0.0419	27.4	4.71	0.0305	20.3	5.28	0.0364
CED[b] (MJ)	463	73.6	0.516	198	34.1	0.221	54.1	14.1	0.0971
HT[ab] (kg 1,4-DCB eq)	2.47	0.39	0.00271	3.62	0.62	0.00403	1.86	0.48	0.00334

[a]*Calculated by ReCiPe v13.1*; MJ = megajoules. [b]*Calculated in SimaPro v8*; 1,4-DCB = 1,4-Dichlorobenzene.

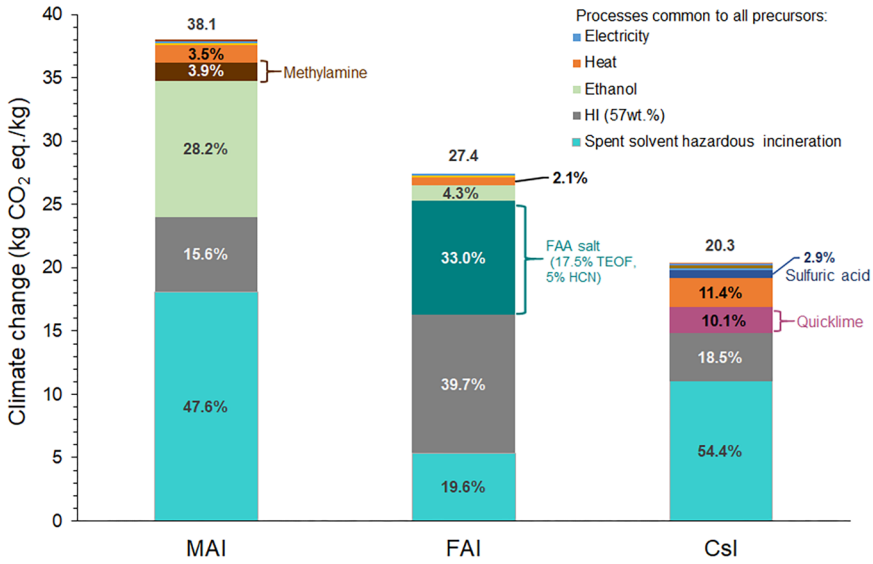

Figure 2. Process contribution analysis for the climate change impact category for the production of perovskite cationic precursors: MAI, FAI, and CsI.

year may be required. If the demand is high enough (thousands of tonnes per year), solar manufacturers or their chemicals contractors might need to build a continuous production facility for steady precursor supply. However, that would require LHP PV to exceed the total current PV market. For the foreseeable future, intermittent batch processing is sufficient for near-term installations.

Life Cycle Impact Assessment (LCIA) of Perovskite Cationic Precursors. Table 1 shows the life cycle impact results for selected midpoint categories across three relevant functional units based on mass, moles, and module area for the studied perovskite cationic precursors. The life cycle material and energy inventory inputs along with emissions and waste allocations entries for the production of MAI, CsI, and FAI are shown in Tables S7, S9, and S15, respectively. Climate change and HT values for upscaled production processes are similar across all three salts (within a factor of 2 or less). Climate change impact is slightly worse for MAI than for CsI and FAI. HT is highest for FAI, followed by MAI and CsI. The CED category has the highest observed difference between precursors, with MAI standing out for its undesirably high embodied energy.

Figure 2 shows a process contribution analysis on a kg basis for the climate change impact category (see Figures S7 and S8 for CED and HT, respectively). In the subsequent sections, we outline the modeling approach for each precursor and its material and energy contributions to LCIA results.

Methylammonium Iodide (MAI). *MAI Synthesis Route and Process Scale Up.* We modeled a process with a capacity of 647 kg per year of MAI to supply a 100 MWp market. The block flow diagram (BFD) showing the process units, mass and energy flows, and waste allocation is shown in Figure S2 along with technical details outlining the calculation of material and energy flows. We scaled up a synthesis route described by Lee et al.[64] that involves the reaction between excess methylamine, dissolved in an anhydrous ethanol solution, and hydroiodic acid under a nitrogen atmosphere and at room temperature. The process yield for this reaction exceeds 90%. The reaction is highly exothermic with a standard enthalpy of reaction of −204.23 kJ/mol. Alternative process routes in the literature report carrying out the reaction at 0 °C for 2 h.[65] We selected the process route by Lee et al. because it is usually more cost-effective and a more standardized operating procedure in industrial settings to use gas purging and cooling to control an exothermic reaction rather than to run the reaction at low temperatures. From a safety viewpoint, gas purging at large scale controls the flammability of methylamine.[66] In this reaction case, removal of excess heat during reaction is also important to maintain high yield and preserve the MAI crystal structure.[67]

MAI Life Cycle Impact Assessment and Process Contribution Analysis. The climate change impact of producing 1 kg of MAI at industrial scale is 38.1 kg CO_2 eq, which is double the impact of producing 1 kg of cadmium telluride (CdTe) semiconductor grade salt (15.6 kg CO_2 eq in ecoinvent). The CED is 463 MJ/kg and the HT is 2.47 kg 1,4-DCB-eq/kg. The rest of ReCiPe midpoint indicators for all impact categories for MAI are in Table S8. The most affected environmental impact category is fossil depletion that has a score of 10.3 kg of oil-eq per kg of MAI. This is caused by the large usage of ethanol

https://dx.doi.org/10.1021/acssuschemeng.0c05619
ACS Sustainable Chem. Eng. 2020, 8, 16537−16548

solvent in the reaction step which places significant demand on the upstream oil and gas mining operations in the life cycle.

Figure 2 shows the contribution of each major process to the climate change impact category. Incineration of spent solvents contributed almost ∼48% of the total impacts. The second highest contributor was the use of ethanol for methylamine solvation and as a reaction medium, which combined amounted to ∼28% of the impacts. The third highest contributor was hydroiodic acid (57 wt % HI) production (∼15.6% of total impacts), particularly the natural gas furnace operations in upstream hydrazine production (Figure S1). The direct heat and electricity for MAI generation contributed only ∼4% of the total impacts.

Formamidinium Iodide (FAI). *FAI Synthesis Route and Precursor Supply Chain.* A production capacity of 655 kg of FAI is needed per year for 100 MWp. The block flow diagram (BFD) of the FAI production process is shown in Figure S3. The process scale-up calculations were based on the synthesis route reported by Eperon et al.[68] that involves the reaction of formamidinium acetate (FAA) salt with 57 wt % hydroiodic acid (HI) at process conditions like those employed in MAI synthesis.

Formamidinium acetate, also commonly known commercially as methanimidamide acetate, is an organic amidine salt that has applications in drug synthesis research. The only synthesis route for FAA salt, reported by one patent and two literature articles in Reaxys database, involves reacting liquid triethyl orthoformate (TEOF) with glacial acetic acid under ammonia refluxing at 135 °C for 45 min (Figure S4 and Table S11).[69−71] The yield is 84.2%. The procedures report cooling operations that indicate the exothermicity of reaction, but the exact heat of reaction could not be calculated due to missing physiochemical data about the specific enthalpy of formation of the FAA salt. LCI of TEOF was developed separately because it is not available in existing LCA databases. We modeled a process to produce 615 kg of TEOF following the commercial synthesis route involving the reaction between hydrocyanic acid (HCN) and anhydrous ethanol under dry hydrogen chloride (HCl) in petroleum ether solvent at subzero conditions (−15 °C)[72,73] (Figure S5 and Table S13).

FAI Life Cycle Impact Assessment and Process Contribution Analysis. FAI has climate change impact of 27.4 kg CO_2 eq., CED of 198 MJ and HT of 3.62 kg 1,4 DCB-equivalent per kg of FAI. All impact categories calculated by ReCiPe midpoint indicators are reported in Table S10. Figure 2 shows that the highest contributor to the climate change effect is the large material usage of excess hydroiodic acid (57 wt % HI) that is required for complete conversion of the FAA salt, constituting almost 40% of the total climate change impact. The second highest contributor is the use of FAA salt, at 33% of total impacts, especially the upstream HCN production process used to produce TEOF (∼5% of total climate change impacts). The third highest contribution is from the spent solvent incineration which constitutes about 20% of the total impacts. The direct heat and electricity consumption contribute a total of only 1.7% of the total impacts. This result contradicts that of a previous study that estimated a dramatically greater electricity and heat consumption for the FAI production process (∼198 kWh/kg compared to 0.352 kWh/kg of FAI reported here), driven largely by the final drying stage at vacuum for 24 h.[30,74] We are skeptical that such an energy intensive drying process would be performed on an industrial scale, especially given that it is not necessary in the synthesis we analyzed here. Even on laboratory scale, the drying step should be expected to be similar for both MAI and FAI given that the same solvents are employed in synthesis.

Cesium Iodide (CsI). *Cesium Extraction and Refining.* Current commercial reserves of cesium are found as cesium oxide in pollucite ore ($Cs(AlSi_2O_6)$, which contains 29−34% cesium oxide (Cs_2O), depending on mining location.[75,76] Pollucite ore is mined as a byproduct of the lithium mineral lepidolite. Three possible production pathways for recovering cesium salts from cesium ores are direct reduction with metals, decomposition with bases, and acid digestion.[33,77] Acid digestion of pollucite ore is the preferred commercial process. No LCI of cesium ores or compounds is present in commercial LCA databases to date. We scaled up the process for ore digestion by sulfuric acid described by the patent published by Cabot Corporation, the largest cesium ore refiner in the world.[78] The process involves using a 45 wt % sulfuric acid to dissolve the pollucite ore in a calculated ratio of 0.36 kg of ore per 1 L of acid at 115 °C for 16 h (Figure S6 and Table S15).[79] Other auxiliary chemicals (e.g., soda ash and lime) are used for slaking, polishing, and neutralization of excess acids. Further purification steps are required to separate the cesium salt from the insoluble cesium alum. Our calculations indicate that 3.03 kg of pollucite ore is required to produce 1 kg of pure CsI salt, assuming that the average cesium oxide content in pollucite ore is 29.7% (see SI for sample calculations). The acid digestion process produces waste gypsum, slag, and aluminum hydroxide waste. These waste streams can be reused in the construction industry and therefore sent off for further reuse allowing for waste allocation cutoff in our model.[80] The spent sulfuric acid waste is sent to incineration as per EPA regulations. A more optimistic scenario involves distilling the spent solvents under a vacuum and reintegrating them into the process; however, this step may be unlikely due to the presence of heavy metals. Further details are discussed in the section Hotspot Analysis for Solvent Recovery below.

CsI Life Cycle Impact Assessment and Process Contribution Analysis. CsI has a climate change impact of 20.3 kg of CO_2 eq , CED of 54.4 MJ, and 1.86 kg 1,4 DCB-eq per kg of CsI. The ReCiPe midpoint impact categories are reported in Table S16. The process contribution analysis, Figure 2, shows that the incineration of spent sulfuric acid waste accounts for 54.4% of the climate change impact. The second and third highest contributions are from hydroiodic acid (57 wt % HI) usage and direct process heat operations, respectively. The process is heat intensive (∼23.4 MJ per 1 kg of CsI) due to the long reactor operation time (16 h) at elevated temperature and the multiple heating steps incurred during reslurrying and slaking.

Availability of Cesium and Rubidium Minerals. Cesium and rubidium minerals are listed in the top 35 critical minerals of U.S. supply.[75] Cesium is used in a quantity of few thousand kilograms per year in U.S.,[76] most commonly in the form of solutions used in oilfield drilling applications, petroleum cracking, and battery electrolytes. On a much smaller scale, rubidium is mostly used in the production of specialty glasses and a few other applications.

Rubidium has the second largest atomic radius of any monovalent cation, after cesium, and has been used in some efficient and stable LHP PVs.[81,82] Rubidium is comined from similar deposits of cesium and lithium, but in much smaller quantities, obtained as a byproduct from refining cesium and lithium from their ores.[75] It remains uneconomical to

https://dx.doi.org/10.1021/acssuschemeng.0c05619
ACS Sustainable Chem. Eng. 2020, 8, 16537−16548

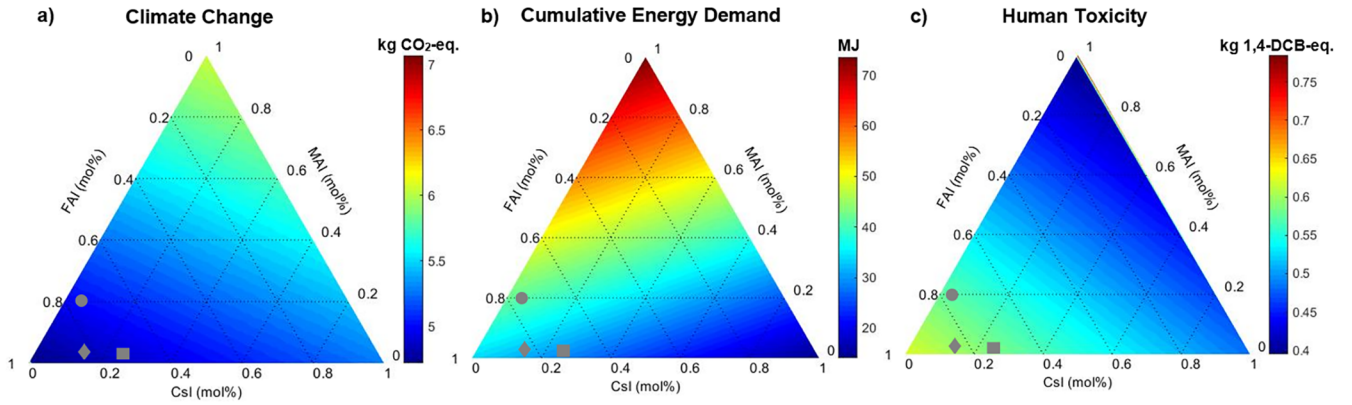

Figure 3. Life cycle impact assessment results across the entire ternary phase space for 1 mol of A-site perovskite precursor compositions for (a) Climate change, (b) Cumulative energy demand, (c) Human toxicity. Formulation symbols: (circles) $Cs_{0.10}MA_{0.15}FA_{0.75}$, (squares) $Cs_{0.25}FA_{0.75}$, and (diamonds) $Cs_{0.15}FA_{0.85}$.

exclusively mine for rubidium due to its very low concentration in deposits. Therefore, rubidium does not have any availability advantage over cesium for large scale deployment of renewable energy applications.

Our calculations indicate that only 1.8% of current known cesium reserves would be needed to meet the entire U.S. solar PV electricity generation goal for 2022−2050[36] exclusively with $CsPbX_3$-based LHP PVs. Only 0.3% would be needed for state-of-the-art alloys with 15% Cs in the A-site and far less than that considering the current dominant market share of silicon PV. Our calculations are based on the current commercial proven cesium reserves, which are estimated at ∼90,000 t.[83] The 2020 U.S. Mineral Commodity reports estimated the total original worldwide cesium reserves to be ∼220,000 t, mainly present in Canada, Zimbabwe, Namibia, Australia, and Argentina. These cesium reserves are estimated based on the occurrence of pollucite ore. Additional commercial cesium supplies are expected to be available. For example, the Taron project in Argentina is reported to have rich Cs-pharmacosiderite ore deposits, and production phase is expected to begin in the next few years.[84,85] To date, the world's supply of cesium mainly comes from remaining stocks in Tanco mines, Manitoba, Canada with estimated *original* known reserve of 120,000 t of cesium oxide present in ore.

Given our high-end assumptions about near-future cesium use in LHP devices, we believe that cesium availability concerns should not affect the decision to deploy perovskite photovoltaics. LHP PVs will not disrupt the cesium supply chain because so little Cs is required. However, competing demand for cesium from multiple industries, especially oilfield drilling, could all together place constraints on midterm supply.[86]

Life Cycle Impact Assessment of Mixed Cation Perovskite Films. In the previous section we reported environmental impacts of MAI, FAI, and CsI on a 1 kg basis that are relevant from the prospective of their manufacturing. Here, we report impact assessment results of the precursor salts and their alloys per mole to provide useful feedback to solar PV researchers. Figure 3 shows impacts for climate change, CED, and HT per 1 mol of cationic alloy composition across the ternary phase space, including symbols highlight three promising formulations for commercialization mentioned above.

Climate Change. The variation between all compositions in the phase space is less than 30% for the climate change impact category. MAI has the highest climate change impact of 6.05 kg CO_2 eq per mole. FAI and CsI have climate change impacts of 4.71 and 5.28 kg CO_2 eq per mole, respectively. We note that the order of impacts from highest to lowest changed when comparing per mole versus per mass basis because of different molecular weights. In the comparison on a per-mole basis, CsI entails higher climate change effect than FAI, because CsI is more dense than FAI, while MAI remains the highest. The Cs/FA composition space has the lowest impact region.

Cumulative Energy Demand. The CED indicator shows a sizable difference in the energy requirements across formulations. MAI, FAI, and CsI incur 463, 198, and 54.1 MJ per 1 mol, respectively. The CED score is much higher for organic cations, especially MAI-based formulations, than for CsI. The hotspot analysis of energy consumption shows that the large solvent usage in MAI production increases demand for upstream ethylene production process, making the nonrenewable fossil category the highest among all other energy consumption categories. For FAI production, upstream hydrogen cyanide production process for TEOF production is the main source of energy consumption. CED of MAI may be reduced by replacing or recycling the ethanol solvent.

Human Toxicity. The HT impacts for MAI, FAI, and CsI are 0.393, 0.623, and 0.483 kg 1,4-DCB-eq per one mole of cation, respectively. Figure 3c shows that the toxicity increases with increasing fraction of FAI in the perovskite formulation. The difference between the highest and lowest impact across potential commercial compositions is only ∼4.4%. Usage of excess hydroiodic acid in direct FAI synthesis and acetic acid in FAA synthesis carries the largest contribution to HT of FAI. These processes entail upstream lignite mining, and treatment of waste thereof, for heat production, which is associated with considerable human health and ecotoxicity hazards. A possible way to reduce HT impacts for FAI is to reduce the raw material consumption by reducing the usage of or recycling acetic acid and hydroiodic acid. We used USEtox model to distinguish between human health and ecotoxicity.

Figure 4 shows USEtox toxicity contributions for one mole of cationic precursor. FAI has almost twice the impacts of MAI in the terrestrial ecotoxicity and human toxicity- noncancer categories. MAI has the highest impact in human toxicity-

https://dx.doi.org/10.1021/acssuschemeng.0c05619
ACS Sustainable Chem. Eng. 2020, 8, 16537−16548

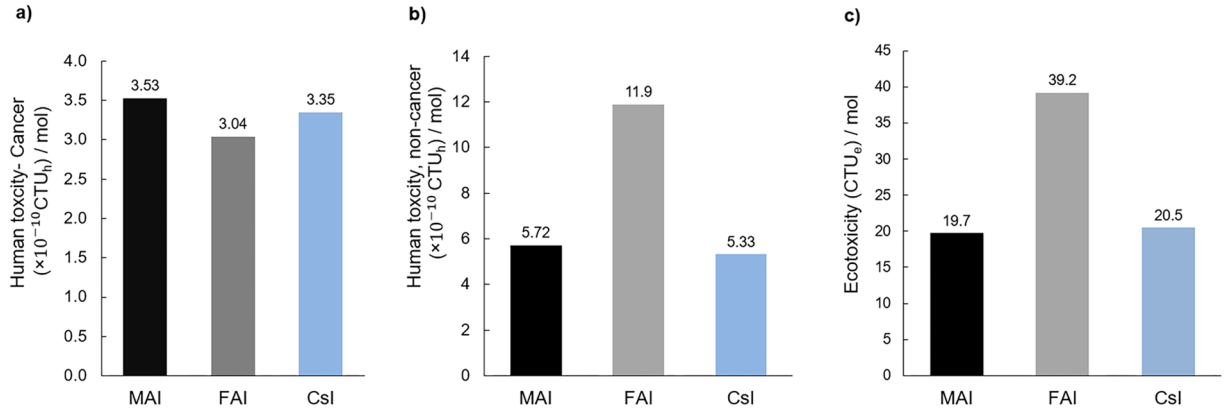

Figure 4. Toxicity performance of MAI, FAI and CsI on per-mole basis using USEtox model across toxicity categories: (a) Human Toxicity-Cancer (HT-cancer), (b) Human Toxicity- noncancer (HT- noncancer), (c) Terrestrial Ecotoxicity.

cancer category, but the impact in this category of all three salts is similar to within ∼20%.

Hotspot Analysis for Solvent Recovery. MAI production uses more solvent than production of FAI and CsI. The large ethanol solvent use and its subsequent incineration are the underlying reasons why MAI carries the highest impacts in climate change, CED, and human toxicity-cancer categories. Recycling of the solvents used in precursor synthesis could reduce the environmental burdens associated with the supply chain of all precursor salts. Here, we consider the sensitivity of impact assessment results to solvent usage and disposal. For small scale, intermittent production capacity, recovering synthesis solvents might not be economically or technically feasible. However, if the LHP PV capacity increases to capture a sizable fraction of the market, precursor production might need to transition to a continuous process with more significant volumes of solvent required. In that case, it is important to note some technical challenges associated with solvent recovery for each cationic precursor.

For MAI production, our calculations indicate that a quantity of ∼8.5 kg of ethanol solvent per 1 kg of MAI is needed for methylamine solvation and recrystallization steps. Spent solvent effluents from unit operations would likely contain a ternary mixture of ethanol, water, and methylamine. A possible recovery route could consist of desorbing methylamine first followed by azeotropic distillation of ethanol/water mixture. However, this operation seems unlikely due to high costs of specialized separations systems for batch scales.

The spent sulfuric acid mixtures from CsI production (∼5.6 kg/kg of CsI) possess a greater environmental hazard because they contain heavy metals (i.e., Cd, Pb) from the ore extraction process. The acidic waste stream also brings the hazard of acid mine drainage.[87,88] Ion exchange and solvent extraction technologies are among a few promising technologies that are still under research and optimization.[89,90] Another option is to collect and send the spent acid stream to existing spent acid treatment operations.[91,92]

The FAI production process and the production of its associated precursors have more potential for the recovery of their spent solvents. Recovery of spent petroleum ether solvent in TEOF production is already reported and modeled in this study.[93] The reactor effluent from FAA production is composed mainly of ethanol byproduct with some ethyl acetate forming an azeotropic mixture and unreacted acetic acid. Finally, FAI production produces a spent solvent mixture composed of unreacted hydroiodic acid, acetic acid byproduct, water, and traces of some alkyl iodides. Presence of high concentrations of hydrogen iodide could lead to difficulty in mixture separation.[94] Use of additives could improve the separation yield of the process.[95]

In our study, solvent recovery was only considered for FAA production since its simple distillation operation can be applied relatively easily in a small batch setting. We assumed that the solvent recovery equipment is available. Building specialized equipment might offset the benefit of solvent recovery in FAA case for such a small scale employed. To carry out this sensitivity calculation, we estimated the distillation utilities (i.e., steam, cooling water), electricity consumption, and nitrogen purging and reduced fresh ethanol usage by the amount of solvent recovered.[96,97] We considered the climate change impact category, with a FU of 1 mol of cationic precursor. Figure 5 shows a comparison of the climate change impacts of the different perovskite alloy formulations with and without solvent recovery (see Table S19 and Table S20 for the rest of midpoint impact categories).

Our results indicate that all formulations lie within a reasonably small range on a molar basis. FAI may offer opportunities for solvent recovery that are not practical for MAI and CsI, reducing climate change impact of cation precursor manufacture by 6−8% for FA-based compositions.

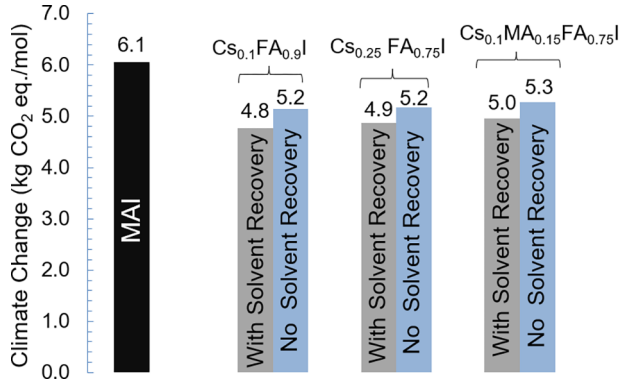

Figure 5. Climate change impact category (kg CO_2 eq) per 1 mol of MAI and selected mixed cation perovskite precursor formulations synthesized with and without solvent recovery in FAA production process.

https://dx.doi.org/10.1021/acssuschemeng.0c05619
ACS Sustainable Chem. Eng. 2020, 8, 16537−16548

Table 2. Comparison of Climate Change, Cumulative Energy Demand, and Human Toxicity Environmental Impacts between Canonical $MAPbI_3$, Mixed Cation $Cs_{0.25}FA_{0.75}PbI_3$, Solar Glass, and PET Flexible Web (Substrate) That May Be Included in Manufacturing 1 m^2 of Perovskite Photovoltaics

Perovskite module component	$MAPbI_3$[a]	$Cs_{0.25}FA_{0.75}PbI_3$[a]	Solar glass[b]	PET flexible web[c]
Amount required per 1 m^2 panel (kg/m^2)	4.29×10^{-3}	4.32×10^{-3}	15.0	0.24
Climate change per 1 kg of material (kg CO_2 eq./kg)[d,e]	15.9	13.3	1.00	279
Climate change of materials per 1 m^2 of module (kg CO_2 eq./m^2)[d,e]	6.82×10^{-2}	5.74×10^{-2}	15.0	0.67
CED per 1 kg of material (MJ/kg.)	150	74.5	0.492	2.11
CEC of materials per 1 m^2 of module (MJ/m^2)[d,e]	0.646	0.322	7.38	0.506
Human toxicity per 1 kg of material (kg 1,4-DCB eq./kg)	1.99	2.18	0.136	0.68
Human toxicity per 1 m^2 of module (kg 1,4-DCB eq./m^2)	8.54×10^{-3}	9.43×10^{-3}	2.04	0.163

[a]Only precursor salts considered. [b]Assuming 2 sheets for front and back of the panel, 3 mm each; see Tables S3 and S4. [c]Assuming a thickness of 175 μm. [d]Calculated by ReCiPe v13.1. [e]Calculated in SimaPro v8.

Comparison to Other Precursors and Module Components. To this point, we have shown comparative analyses of impacts for different cation compositions. We now place those results in context by comparison to other components required for PV module manufacturing. The perovskite film formation involves the reaction between the A-site precursor salt and lead halide salts (i.e., PbI_2 and $PbBr_2$) during either solution or vapor deposition. Lead toxicity has triggered concerns about sustainability of LHP PV systems, but our prior study concluded that the intensity and toxicity potential attributed to possible catastrophic release of lead are less than those from other life cycle stages and less than representative U.S. grid mixes, under reasonable commercialization scenarios.[31] Gong et al. modeled LCI for upscaled PbI_2 commercial production,[42] and we compiled this inventory (Table S17) and ran LCIA using ReCiPe v1.13 protocol. Our results show that PbI_2 has climate change impact of 3.85 kg CO_2 eq , CED of 19.7 MJ, and human toxicity of 0.844 kg 1,4-DCB-eq per 1 mol of PbI_2. The A-site precursor salts and lead iodide salt bear similar impacts on a molar basis.

The perovskite absorber layer is sandwiched between organic or inorganic electron and hole transport layers, which are interfaced with front and back contact layers. We have not calculated impacts from those layers because the industry has not yet unified around optimal materials for these layers and research suggests that comparatively high-impact options such as spiro-OMe-TAD can likely be replaced with simple oxides or small organic molecules.[98] Since no commercial device stack has been publicized, the results of preliminary LHP PV LCA studies are speculative and depend on their assumptions of device architectures, material selection, and deposition approaches.[99]

All layers are deposited on glass or flexible plastic (e.g., PET) substrates, although devices on PET would likely need to be encapsulated in glass for stability reasons. Glass substrates incur a much larger climate change impact than the precursors for the perovskite layer because of the large mass required. Table 2 compares mass and environmental impacts of the combined perovskite precursors (AI + PbI_2), glass, and PET required per area for module manufacturing. Assuming two glass sheets with typical thickness of 3 mm and glass density of 2500 kg/m^3, 15 kg/m^2 is needed for modules. Low-iron flat glass has climate change impact of 1.0 kg CO_2-eq/kg (ecoinvent), resulting in 15 kg CO_2-eq/m^2. In comparison, $Cs_{0.25}FA_{0.75}PbI_3$ has a climate change impact *per mass* of 13.3 kg CO_2-eq/kg that is much larger than glass, but only ~4.32 g/m^2 is needed for micron film thickness, resulting in climate change effect of only 0.0574 kg CO_2 eq/m^2. The impact per module area is therefore over 1000x higher for glass than for the total perovskite chemical precursor salts. For a thin flexible PET substrate, a thickness of 175 μm is needed.[100] Assuming a density of 1380 kg/m^3, a value of 0.24 kg/m^2 is needed with climate change impact of 0.67 kg CO_2-eq/m^2. Although the impacts of PET substrates are significantly less than glass, the need for glass encapsulation to act as an environmental barrier might negate this benefit. Similar results hold regarding relative magnitudes of CED and human toxicity between module components. The key findings that impacts are similar across perovskite compositions and that other module components have orders of magnitude larger impacts than the perovskite precursors indicate that environmental impact should not play a key role in selection of perovskite composition, which can then be completely driven by PV efficiency and stability.

CONCLUSIONS

This study showed that the environmental impacts of mixed cation perovskite alloys and archetypal MA-based perovskite formulation are similar. The results of this study contradict the conclusions of a previous study that warned of outsized environmental impacts of FA, which is used in mixed perovskite alloys with the best PV performance. We believe that the previous study overestimated the energy consumption of the manufacturing processes of perovskite cationic precursor salt production in their life cycle inventory (LCI) models by choosing lab-scale conditions over process engineering assumptions routinely employed in the chemicals industry. Our study focused on the impacts of production of the perovskite precursor salts, without convoluting these results with impacts from their processing into films, which may not yet be optimized.

By the employment of process design concepts to scale-up perovskite precursor salts provided, we posit that a more accurate impact assessment was obtained. The largest process contribution for improving supply chain sustainability of perovskite cation precursor salts changed from electricity consumption to solvent usage for industrial-scale models in comparison to lab-scale models.

Cesium criticality concerns should not hinder the selection of optimal perovskite compositions or the scalability of perovskite PV deployment. Only 0.3% of current proven cesium reserves would be required to meet the entire U.S. net electricity generation goals solely with LHP PV systems from 2022 to 2050 for mixed cationic perovskite formulation.

Finally, we conclude that perovskite film compositions should be selected solely based on efficiency and stability. There are no significant differences in environmental impacts

https://dx.doi.org/10.1021/acssuschemeng.0c05619
ACS Sustainable Chem. Eng. 2020, 8, 16537−16548

between A-site cation formulations, and the impacts between cationic precursors and lead iodide are all similar to each other across climate change, human toxicity, and cumulative energy demand on a molar basis. A complete LCA study of the entire scaled-up perovskite module manufacturing process should be carried out as soon as such commercially viable processes and device architectures are communicated. However, it is already clear that the impacts of perovskite precursors are orders of magnitude lower than those of other module components such as glass. The commercial-scale LCI models for perovskite precursor salts provided by this study might aid in more transparent and robust environmental analysis that can contribute to sustainable design and manufacturing of LHP photovoltaics.

■ ASSOCIATED CONTENT

Supporting Information

The Supporting Information is available free of charge at https://pubs.acs.org/doi/10.1021/acssuschemeng.0c05619.

LCI data sets, block flow diagrams, sample calculations, and tables of impact results (PDF)

■ AUTHOR INFORMATION

Corresponding Author

Jason B. Baxter − *Department of Chemical and Biological Engineering, Drexel University, Philadelphia, Pennsylvania 19104, United States;* orcid.org/0000-0001-8702-3915; Email: jbaxter@drexel.edu

Authors

Sherif A. Khalifa − *Department of Chemical and Biological Engineering, Drexel University, Philadelphia, Pennsylvania 19104, United States*

Sabrina Spatari − *Department of Civil, Architectural, and Environmental Engineering, Drexel University, Philadelphia, Pennsylvania 19104, United States; Faculty of Civil and Environmental Engineering, Technion − Israel Institute of Technology, Haifa 3200002, Israel;* orcid.org/0000-0001-7243-9993

Aaron T. Fafarman − *Department of Chemical and Biological Engineering, Drexel University, Philadelphia, Pennsylvania 19104, United States;* orcid.org/0000-0003-3652-3383

Complete contact information is available at: https://pubs.acs.org/10.1021/acssuschemeng.0c05619

Notes

The authors declare no competing financial interest.

■ ACKNOWLEDGMENTS

The authors acknowledge support from NSF grant CBET-1704957.

■ REFERENCES

(1) Photovoltaics Report - Fraunhofer ISE https://www.ise.fraunhofer.de/en/publications/studies/photovoltaics-report.html (accessed Jan 19, 2020).

(2) Global solar may reach 8,500 GW by 2050 − IRENA − pv magazine International https://www.pv-magazine.com/2019/04/09/global-solar-may-reach-8500-gw-by-2050-irena/ (accessed Jan 19, 2020).

(3) Green, M. A.; Dunlop, E. D.; Hohl-Ebinger, J.; Yoshita, M.; Kopidakis, N.; Ho-Baillie, A. W. Y. Solar Cell Efficiency Tables (Version 55). *Prog. Photovoltaics* **2020**, *28* (1), 3−15.

(4) Jung, E. H.; Jeon, N. J.; Park, E. Y.; Moon, C. S.; Shin, T. J.; Yang, T. Y.; Noh, J. H.; Seo, J. Efficient, Stable and Scalable Perovskite Solar Cells Using Poly(3-Hexylthiophene). *Nature*. Nature Publishing Group March 28, 2019; pp 511−515. DOI: 10.1038/s41586-019-1036-3.

(5) Kojima, A.; Teshima, K.; Shirai, Y.; Miyasaka, T. Organometal Halide Perovskites as Visible-Light Sensitizers for Photovoltaic Cells. *J. Am. Chem. Soc.* **2009**, *131* (17), 6050−6051.

(6) Extance, A. The Reality behind Solar Power's next Star Material. *Nature*. NLM (Medline) June 1, 2019; pp 429−432. DOI: 10.1038/d41586-019-01985-y.

(7) Rajagopal, A.; Yao, K.; Jen, A. K. Y. Toward Perovskite Solar Cell Commercialization: A Perspective and Research Roadmap Based on Interfacial Engineering. *Adv. Mater.* **2018**, *30* (32), 1800455−45.

(8) Li, Z.; Klein, T. R.; Kim, D. H.; Yang, M.; Berry, J. J.; van Hest, M. F. A. M.; Zhu, K. Scalable Fabrication of Perovskite Solar Cells. *Nature Reviews Materials* **2018**, *3*. DOI: 10.1038/natrevmats.2018.17.

(9) Rajagopal, A.; Yang, Z.; Jo, S. B.; Braly, I. L.; Liang, P.-W.; Hillhouse, H. W.; Jen, A. K.-Y. Highly Efficient Perovskite-Perovskite Tandem Solar Cells Reaching 80% of the Theoretical Limit in Photovoltage. *Adv. Mater.* **2017**, *29* (34), 1702140.

(10) Forgács, D.; Gil-Escrig, L.; Pérez-Del-Rey, D.; Momblona, C.; Werner, J.; Niesen, B.; Ballif, C.; Sessolo, M.; Bolink, H. J. Efficient Monolithic Perovskite/Perovskite Tandem Solar Cells. *Adv. Energy Mater.* **2017**, *7* (8), 1602121.

(11) Eperon, G. E.; Leijtens, T.; Bush, K. A.; Prasanna, R.; Green, T.; Wang, J. T. W.; McMeekin, D. P.; Volonakis, G.; Milot, R. L.; May, R.; Palmstrom, A.; Slotcavage, D. J.; Belisle, R. A.; Patel, J. B.; Parrott, E. S.; Sutton, R. J.; Ma, W.; Moghadam, F.; Conings, B.; Babayigit, A.; Boyen, H. G.; Bent, S.; Giustino, F.; Herz, L. M.; Johnston, M. B.; McGehee, M. D.; Snaith, H. J. Perovskite-Perovskite Tandem Photovoltaics with Optimized Band Gaps. *Science* **2016**, *354* (6314), 861−865.

(12) Duong, T.; Wu, Y.; Shen, H.; Peng, J.; Fu, X.; Jacobs, D.; Wang, E.-C.; Kho, T. C.; Fong, K. C.; Stocks, M.; Franklin, E.; Blakers, A.; Zin, N.; McIntosh, K.; Li, W.; Cheng, Y.-B.; White, T. P.; Weber, K.; Catchpole, K. Rubidium Multication Perovskite with Optimized Bandgap for Perovskite-Silicon Tandem with over 26% Efficiency. *Adv. Energy Mater.* **2017**, *7* (14), 1700228.

(13) Werner, J.; Niesen, B.; Ballif, C. Perovskite/Silicon Tandem Solar Cells: Marriage of Convenience or True Love Story? − An Overview. *Adv. Mater. Interfaces* **2018**, *5* (1). 1700731.

(14) Tan, W.; Bowring, A. R.; Meng, A. C.; McGehee, M. D.; McIntyre, P. C. Thermal Stability of Mixed Cation Metal Halide Perovskites in Air. *ACS Appl. Mater. Interfaces* **2018**, *10* (6), 5485−5491.

(15) Senocrate, A.; Yeong, G.; Maier, J.; Kim, G. Y.; Grätzel, M.; Maier, J.; Yeong, G.; Maier, J. Thermochemical Stability of Hybrid Halide Perovskites. *ACS Energy Letters* **2019**, *6* (12), 70569.

(16) Bush, K. A.; Frohna, K.; Prasanna, R.; Beal, R. E.; Leijtens, T.; Swifter, S. A.; McGehee, M. D. Compositional Engineering for Efficient Wide Band Gap Perovskites with Improved Stability to Photoinduced Phase Segregation. *ACS Energy Lett.* **2018**, *3* (2), 428.

(17) Jeon, N. J.; Noh, J. H.; Yang, W. S.; Kim, Y. C.; Ryu, S.; Seo, J.; Seok, S. il. Compositional Engineering of Perovskite Materials for High-Performance Solar Cells. *Nature* **2015**, *517* (7535), 476−480.

(18) Juarez-Perez, E. J.; Ono, L. K.; Maeda, M.; Jiang, Y.; Hawash, Z.; Qi, Y. Photodecomposition and Thermal Decomposition in Methylammonium Halide Lead Perovskites and Inferred Design Principles to Increase Photovoltaic Device Stability. *J. Mater. Chem. A* **2018**, *6* (20), 9604−9612.

(19) Han, Y.; Meyer, S.; Dkhissi, Y.; Weber, K.; Pringle, J. M.; Bach, U.; Spiccia, L.; Cheng, Y. B. Degradation Observations of Encapsulated Planar CH3NH3PbI3 Perovskite Solar Cells at High Temperatures and Humidity. *J. Mater. Chem. A* **2015**, *3* (15), 8139−8147.

(20) Jung, E. H.; Jeon, N. J.; Park, E. Y.; Moon, C. S.; Shin, T. J.; Yang, T. Y.; Noh, J. H.; Seo, J. Efficient, Stable and Scalable Perovskite Solar Cells Using Poly(3-Hexylthiophene). *Nature*. Nature

Publishing Group March 28, 2019; pp 511−515. DOI: 10.1038/s41586-019-1036-3.
(21) Saliba, M.; Matsui, T.; Seo, J.-Y. Y.; Domanski, K.; Correa-Baena, J.-P. P.; Nazeeruddin, M. K.; Zakeeruddin, S. M.; Tress, W.; Abate, A.; Hagfeldt, A.; Grätzel, M.; Khaja, M. Cesium-Containing Triple Cation Perovskite Solar Cells: Improved Stability, Reproducibility and High Efficiency. *Energy Environ. Sci.* **2016**, *9* (6), 1989−1997.
(22) Palmstrom, A. F.; Eperon, G. E.; Leijtens, T.; Prasanna, R.; Habisreutinger, S. N.; Nemeth, W.; Gaulding, E. A.; Dunfield, S. P.; Reese, M.; Nanayakkara, S.; Moot, T.; Werner, J.; Liu, J.; To, B.; Christensen, S. T.; McGehee, M. D.; van Hest, M. F. A. M.; Luther, J. M.; Berry, J. J.; Moore, D. T. Enabling Flexible All-Perovskite Tandem Solar Cells. *Joule* **2019**, *3* (9), 2193−2204.
(23) Leijtens, T.; Prasanna, R.; Bush, K. A.; Eperon, G. E.; Raiford, J. A.; Gold-Parker, A.; Wolf, E. J.; Swifter, S. A.; Boyd, C. C.; Wang, H. P.; Toney, M. F.; Bent, S. F.; McGehee, M. D. Tin-Lead Halide Perovskites with Improved Thermal and Air Stability for Efficient All-Perovskite Tandem Solar Cells. *Sustainable Energy and Fuels* **2018**, *2* (11), 2450−2459.
(24) Turren-Cruz, S.-H. H.; Hagfeldt, A.; Saliba, M.; Turren-Cruz, S.-H. H.; Hagfeldt, A.; Saliba, M. Methylammonium-Free, High-Performance and Stable Perovskite Solar Cells on a Planar Architecture. *Science* **2018**, *3583*, eaat3583.
(25) Maranghi, S.; Parisi, M. L.; Basosi, R.; Sinicropi, A. Environmental Profile of the Manufacturing Process of Perovskite Photovoltaics: Harmonization of Life Cycle Assessment Studies. *Energies* **2019**, *12* (19), 3746.
(26) Muteri, V.; Cellura, M.; Curto, D.; Franzitta, V.; Longo, S.; Mistretta, M.; Parisi, M. L. Review on Life Cycle Assessment of Solar Photovoltaic Panels. *Energies* **2020**, *13* (1), 252.
(27) Celik, I.; Song, Z.; Cimaroli, A. J.; Yan, Y.; Heben, M. J.; Apul, D. Life Cycle Assessment (LCA) of Perovskite PV Cells Projected from Lab to Fab. *Sol. Energy Mater. Sol. Cells* **2016**, *156*, 157−169.
(28) Espinosa, N.; Serrano-Luján, L.; Urbina, A.; Krebs, F. C. Solution and Vapour Deposited Lead Perovskite Solar Cells: Ecotoxicity from a Life Cycle Assessment Perspective. *Sol. Energy Mater. Sol. Cells* **2015**, *137*, 303−310.
(29) Ibn-Mohammed, T.; Koh, S. C. L.; Reaney, I. M.; Acquaye, A.; Schileo, G.; Mustapha, K. B.; Greenough, R. Perovskite Solar Cells: An Integrated Hybrid Lifecycle Assessment and Review in Comparison with Other Photovoltaic Technologies. *Renewable and Sustainable Energy Reviews*. Elsevier Ltd December 1, 2017; pp 1321−1344. DOI: 10.1016/j.rser.2017.05.095.
(30) Alberola-Borràs, J. A.; Vidal, R.; Mora-Seró, I. Evaluation of Multiple Cation/Anion Perovskite Solar Cells through Life Cycle Assessment. *Sustainable Energy and Fuels* **2018**, *2* (7), 1600−1609.
(31) Billen, P.; Leccisi, E.; Dastidar, S.; Li, S.; Lobaton, L.; Spatari, S.; Fafarman, A. T.; Fthenakis, V. M.; Baxter, J. B. Comparative Evaluation of Lead Emissions and Toxicity Potential in the Cradle-to-Gate Life Cycle of Lead Halide Perovskite Photovoltaics. *Energy* **2019**, *166*, 1−6.
(32) Gardner, K. L.; Tait, J. G.; Merckx, T.; Qiu, W.; Paetzold, U. W.; Kootstra, L.; Jaysankar, M.; Gehlhaar, R.; Cheyns, D.; Heremans, P.; Poortmans, J. Nonhazardous Solvent Systems for Processing Perovskite Photovoltaics. *Adv. Energy Mater.* **2016**, *6* (14), 1−8.
(33) Federal Register:: Final List of Critical Minerals 2018 https://www.federalregister.gov/documents/2018/05/18/2018-10667/final-list-of-critical-minerals-2018 (accessed Feb 15, 2020).
(34) ISO - ISO 14040:2006 - Environmental management — Life cycle assessment — Principles and framework https://www.iso.org/standard/37456.html (accessed Jan 26, 2020).
(35) ISO 14044:2006(en), Environmental management — Life cycle assessment — Requirements and guidelines https://www.iso.org/obp/ui/#iso:std:iso:14044:ed-1:v1:en (accessed Aug 18, 2018).
(36) EIA - Annual Energy Outlook 2019 https://www.eia.gov/outlooks/aeo/ (accessed Jan 19, 2020).
(37) Huijbregts, M. A. J.; Steinmann, Z. J. N.; Elshout, P. M. F.; Stam, G.; Verones, F.; Vieira, M.; Zijp, M.; Hollander, A.; van Zelm, R. ReCiPe2016: A Harmonised Life Cycle Impact Assessment Method at Midpoint and Endpoint Level. *Int. J. Life Cycle Assess.* **2017**, *22* (2), 138−147.
(38) Frischknecht, R.; Wyss, F.; Büsser Knöpfel, S.; Lützkendorf, T.; Balouktsi, M. Cumulative Energy Demand in LCA: The Energy Harvested Approach. *Int. J. Life Cycle Assess.* **2015**, *20* (7), 957−969.
(39) Rosenbaum, R. K.; Huijbregts, M. A. J.; Henderson, A. D.; Margni, M.; McKone, T. E.; van de Meent, D.; Hauschild, M. Z.; Shaked, S.; Li, D. S.; Gold, L. S.; Jolliet, O. USEtox Human Exposure and Toxicity Factors for Comparative Assessment of Toxic Emissions in Life Cycle Analysis: Sensitivity to Key Chemical Properties. *Int. J. Life Cycle Assess.* **2011**, *16* (8), 710−727.
(40) Fantke, P.; Bijster, M.; Guignard, C.; Hauschild, M. Z.; Huijbregts, Mark, A. J.; Jolliet, O.; Kounina, A.; Magaud, V.; Margni, M.; McKone, T. E.; Posthuma, L.; Rosenbaum, R. K.; van de Meent, D.; van Zelm, R. *USEtox 2.0 Documentation (Version 1)*; Fantke, P., Ed.; USEtox International Center hosted at the Technical University of Denmark, 2017. DOI: 10.11581/DTU:00000011.
(41) Rosenbaum, R. K.; Bachmann, T. M.; Gold, L. S.; Huijbregts, M. A. J.; Jolliet, O.; Juraske, R.; Koehler, A.; Larsen, H. F.; MacLeod, M.; Margni, M.; McKone, T. E.; Payet, J.; Schuhmacher, M.; van de Meent, D.; Hauschild, M. Z. USEtox - The UNEP-SETAC Toxicity Model: Recommended Characterisation Factors for Human Toxicity and Freshwater Ecotoxicity in Life Cycle Impact Assessment. *Int. J. Life Cycle Assess.* **2008**, *13* (7), 532−546.
(42) Gong, J.; Darling, S. B.; You, F. Perovskite Photovoltaics: Life-Cycle Assessment of Energy and Environmental Impacts. *Energy Environ. Sci.* **2015**, *8*, 1953−1968.
(43) Lyday, P. A.; Kaiho, T. Iodine and Iodine Compounds. In *Ullmann's Encyclopedia of Industrial Chemistry*; Wiley-VCH Verlag GmbH & Co. KGaA: Weinheim, Germany, 2015; pp 1−13. DOI: 10.1002/14356007.a14_381.pub2.
(44) Mills, J. F.; Frim, R.; Ukeles, S. D.; Yoffe, D. Bromine. In *Ullmann's Encyclopedia of Industrial Chemistry*; Wiley-VCH Verlag GmbH & Co. KGaA: Weinheim, Germany, 2015; pp 1−20. DOI: 10.1002/14356007.a04_391.pub2.
(45) Carr, D. S. Lead Compounds. In *Ullmann's Encyclopedia of Industrial Chemistry*; Wiley-VCH Verlag GmbH & Co. KGaA: Weinheim, Germany, 2000. DOI: 10.1002/14356007.a15_249.
(46) Geisler, G.; Hofstetter, T. B.; Hungerbühler, K. Production of Fine and Speciality Chemicals: Procedure for the Estimation of LCIs. *Int. J. Life Cycle Assess.* **2004**, *9* (2), 101−113.
(47) Piccinno, F.; Hischier, R.; Seeger, S.; Som, C. From Laboratory to Industrial Scale: A Scale-up Framework for Chemical Processes in Life Cycle Assessment Studies. *J. Cleaner Prod.* **2016**, *135*, 1085−1097.
(48) Tecchio, P.; Freni, P.; de Benedetti, B.; Fenouillot, F. Ex-Ante Life Cycle Assessment Approach Developed for a Case Study on Bio-Based Polybutylene Succinate. *J. Cleaner Prod.* **2016**, *112*, 316−325.
(49) Buyle; Audenaert; Billen; Boonen; van Passel. The Future of Ex-Ante LCA? Lessons Learned and Practical Recommendations. *Sustainability* **2019**, *11* (19), 5456.
(50) Riazi, B.; Karanjikar, M.; Spatari, S. Renewable Rubber and Jet Fuel from Biomass: Evaluation of Greenhouse Gas Emissions and Land Use Trade-Offs in Energy and Material Markets. *ACS Sustainable Chem. Eng.* **2018**, *6* (11), 14414−14422.
(51) Riazi, B.; Zhang, J.; Yee, W.; Ngo, H.; Spatari, S. Life Cycle Environmental and Cost Implications of Isostearic Acid Production for Pharmaceutical and Personal Care Products. *ACS Sustainable Chem. Eng.* **2019**, *7* (18), 15247−15258.
(52) Aspen Plus | Leading Process Simulation Software | AspenTech https://www.aspentech.com/en/products/engineering/aspen-plus (accessed Jul 29, 2020).
(53) SimaPro, version 9.1.0.7; PRe'Consultants: Amersfoort, TheNetherlands, 2020 https://simapro.com/ (accessed Jul 29, 2020).
(54) Ecoinvent 3.5; Swiss Center for Life Cycle Inventories:Duebendorf, Switzerland, 2019 https://www.ecoinvent.org/database/older-versions/ecoinvent-35/ecoinvent-35.html (accessed Jul 29, 2020).

(55) U.S. Life Cycle Inventory Database | NREL https://www.nrel.gov/lci/ (accessed Jan 27, 2020).
(56) Hischier, R.; Hellweg, S.; Capello, C.; Primas, A. Ecoinvent : Materials and Agriculture Establishing Life Cycle Inventories of Chemicals Based on Differing Data Availability. *Int. J. Life Cycle Assess.* **2005**, *10* (Lci), 59−67.
(57) Jiménez-González, C.; Kim, S.; Overcash, M. R. Methodology for Developing Gate-to-Gate Life Cycle Inventory Information. *Int. J. Life Cycle Assess.* **2000**, *5* (3), 153−159.
(58) Parvatker, A. G.; Eckelman, M. J. Comparative Evaluation of Chemical Life Cycle Inventory Generation Methods and Implications for Life Cycle Assessment Results. *ACS Sustainable Chem. Eng.* **2019**, *7* (1), 350−367.
(59) Defining Hazardous Waste: Listed, Characteristic and Mixed Radiological Wastes | Hazardous Waste | US EPA https://www.epa.gov/hw/defining-hazardous-waste-listed-characteristic-and-mixed-radiological-wastes#FandK (accessed Feb 22, 2020).
(60) US EPA, O. Chemical Data Reporting under the Toxic Substances Control Act.
(61) Bruening, K.; Dou, B.; Simonaitis, J.; Lin, Y. Y.; van Hest, M. F. A. M.; Tassone, C. J. Scalable Fabrication of Perovskite Solar Cells to Meet Climate Targets. *Joule* **2018**, *2* (11), 2464−2476.
(62) First Solar, Module data sheet http://www.firstsolar.com/en/Resources/Technical-Documents (accessed Jul 30, 2020).
(63) Turton, R.; Bailie, R.; Whiting, W.; Shaeiwitz, J. *Analysis, Synthesis and Design of Chemical Processes*; **2008**.
(64) Lee, M. M.; Teuscher, J.; Miyasaka, T.; Murakami, T. N.; Snaith, H. J. Efficient Hybrid Solar Cells Based on Meso-Superstructured Organometal Halide Perovskites. *Science* **2012**, *338* (6107), 643−647.
(65) Noh, J. H.; Jeon, N. J.; Choi, Y. C.; Nazeeruddin, M. K.; Grätzel, M.; Seok, S. il. Nanostructured TiO2/CH3NH3PbI3 Heterojunction Solar Cells Employing Spiro-OMeTAD/Co-Complex as Hole-Transporting Material. *J. Mater. Chem. A* **2013**, *1* (38), 11842−11847.
(66) METHYLAMINE, ANHYDROUS Chemical Datasheet | CAMEO Chemicals | NOAA https://cameochemicals.noaa.gov/chemical/8850 (accessed Jul 29, 2020).
(67) Conings, B.; Drijkoningen, J.; Gauquelin, N.; Babayigit, A.; D'Haen, J.; D'Olieslaeger, L.; Ethirajan, A.; Verbeeck, J.; Manca, J.; Mosconi, E.; Angelis, F. D.; Boyen, H.-G. Intrinsic Thermal Instability of Methylammonium Lead Trihalide Perovskite. *Adv. Energy Mater.* **2015**, *5* (15), 1500477.
(68) Eperon, G. E.; Stranks, S. D.; Menelaou, C.; Johnston, M. B.; Herz, L. M.; Snaith, H. J. Formamidinium Lead Trihalide: A Broadly Tunable Perovskite for Efficient Planar Heterojunction Solar Cells. *Energy Environ. Sci.* **2014**, *7* (3), 982−988.
(69) Method for producing formamidine acetate -JP5722560B2 - 20 May 2015. https://patents.google.com/patent/JP5722560B2/en?oq=JP5722560%2c+2015%2c+B2 (accessed Jul 29, 2020).
(70) Taylor, E. C.; Ehrhart, W. A. A Convenient Synthesis of Formamidine and Acetamidine Acetate. *J. Am. Chem. Soc.* **1960**, *82* (12), 3138−3141.
(71) Krechl, J.; Böhm, S.; Smrčková, S.; Kuthan, J. Simple Amidinium Carboxylates - An MO Treatment of Molecular Geometry and Electronic Structure. *Collect. Czech. Chem. Commun.* **1989**, *54* (3), 673−683.
(72) CN103739463A - Simple and convenient method for producing high-purity ortho-formate - 17 November 2017. https://patents.google.com/patent/CN103739463A/en?oq=CN103739463%2c+2017%2c+B (accessed Jul 29, 2020).
(73) Dewolfe, R. H. *Carboxylic Ortho Acid Derivatives : Preparation and Synthetic Applications*.; Elsevier Science, 1970.
(74) Yang, W. S.; Noh, J. H.; Jeon, N. J.; Kim, Y. C.; Ryu, S.; Seo, J.; Seok, S. I. High-Performance Photovoltaic Perovskite Layers Fabricated through Intramolecular Exchange. *Science* **2015**, *348* (6240), 1234.
(75) Cesium and Rubidium Statistics and Information https://www.usgs.gov/centers/nmic/cesium-and-rubidium-statistics-and-information (accessed Feb 12, 2020).
(76) Goyena, R. Cesium Information- National Minerals Information Center. *J. Chem. Inf. Model.* **2019**, *53* (9), 1689−1699.
(77) Bick, M.; Prinz, H.; Steinmetz, A. Cesium and Cesium Compounds. In *Ullmann's Encyclopedia of Industrial Chemistry*; Wiley-VCH Verlag GmbH & Co. KGaA: Weinheim, Germany, 2010. DOI: 10.1002/14356007.a06_153.pub2.
(78) Patrick, M. Brown. US6436879B1 - Process for producing a predetermined cesium compound - 20 August 2002. https://patents.google.com/patent/US6436879B1/en?oq=US+6%2c436%2c879+B1 (accessed Jul 29, 2020).
(79) Pollucite Mineral Data http://webmineral.com/data/Pollucite.shtml#.XZ9dH2YpBhE (accessed May 4, 2020).
(80) Yüksel, İ. A Review of Steel Slag Usage in Construction Industry for Sustainable Development. *Environment, Development and Sustainability*. Springer: Netherlands, April 1, 2017; pp 369−384. DOI: 10.1007/s10668-016-9759-x.
(81) Saliba, M.; Matsui, T.; Domanski, K.; Seo, J.-Y.; Ummadisingu, A.; Zakeeruddin, S. M.; Correa-Baena, J.-P. J.-P. J.-P.; Tress, W. R.; Abate, A.; Hagfeldt, A.; Grätzel, M.; Gratzel, M. Incorporation of Rubidium Cations into Perovskite Solar Cells Improves Photovoltaic Performance. *Science (Washington, DC, U. S.)* **2016**, *354* (6309), 206−209.
(82) Duong, T.; Wu, Y.; Shen, H.; Peng, J.; Fu, X.; Jacobs, D.; Wang, E.-C.; Kho, T. C.; Fong, K. C.; Stocks, M.; Franklin, E.; Blakers, A.; Zin, N.; McIntosh, K.; Li, W.; Cheng, Y.-B.; White, T. P.; Weber, K.; Catchpole, K. Rubidium Multication Perovskite with Optimized Bandgap for Perovskite-Silicon Tandem with over 26% Efficiency. *Adv. Energy Mater.* **2017**, *7* (14), 1700228.
(83) Mineral Commodity Summaries https://www.usgs.gov/centers/nmic/mineral-commodity-summaries (accessed Feb 15, 2020).
(84) Taron Group | Cascadero Copper Corporation https://www.cascadero.com/properties/argentina/taron-group/ (accessed Feb 16, 2020).
(85) Cascadero Copper coporation. US20190048437A1 - Recovery of cesium from epithermal mineral deposits, U.S. Patent, 14 February 2019 https://patents.google.com/patent/US20190048437A1/en (accessed Jul 30, 2020).
(86) Vidal, R.; Alberola-Borràs, J. A.; Mora-Seró, I. Abiotic Depletion and the Potential Risk to the Supply of Cesium. *Resour. Policy* **2020**, *68*, 101792.
(87) Akcil, A.; Koldas, S. Acid Mine Drainage (AMD): Causes, Treatment and Case Studies. *Journal of Cleaner Production*. Elsevier January 1, 2006; pp 1139−1145. DOI: 10.1016/j.jclepro.2004.09.006.
(88) Johnson, D. B.; Hallberg, K. B. Acid Mine Drainage Remediation Options: A Review. *Sci. Total Environ.* **2005**, *338* (1−2), 3−14.
(89) Kesieme, U.; Chrysanthou, A.; Catulli, M.; Cheng, C. Y. A Review of Acid Recovery from Acidic Mining Waste Solutions Using Solvent Extraction. *J. Chem. Technol. Biotechnol.*. John Wiley and Sons Ltd December 1, 2018; pp 3374−3385. DOI: 10.1002/jctb.5728.
(90) Asof, M.; Rachman, S. A.; Nurmawi, W. A.; Ramayanti, C. Recovery of H2SO4 from Spent Acid Waste Using Bentonite Adsorbent. *MATEC Web Conf.* **2017**, *101*, 02007.
(91) MECS® Sulfuric Acid and Environmental Technologies - DuPont Industrial Biosciences http://cleantechnologies.dupont.com/technologies/mecs/ (accessed Feb 20, 2020).
(92) Spent Acid Recovery Process and Plant Design - DuPont Industrial Biosciences http://cleantechnologies.dupont.com/technologies/mecs/technologiestechnologies-mecsdupont-clean-technologies-mecs-processes/mecsr-sulfuric-acid-regeneration-technology/ (accessed Feb 20, 2020).
(93) CN103483165B - Prepare the green cleaning procedure of ortho-formate, Chinese patent, 24 February 2016. https://patents.

https://dx.doi.org/10.1021/acssuschemeng.0c05619
ACS Sustainable Chem. Eng. 2020, 8, 16537−16548

google.com/patent/CN103483165B/en?oq=CN103483165B+ (accessed Jul 30, 2020).
(94) Johnson, W.; Singleton, T.. US3772156A - Purification of acetic acid streams by distillation, U.S. patent, 13 November 1990. https://patents.google.com/patent/US3772156A/en?oq=US3772156A (accessed Jul 30, 2020).
(95) Pagel, H. A.; Toren, P. E.; McLafferty, F. W. Use of Tributyl Phosphate for Separating Acetic Acid from Hydrochloric Acid. *Anal. Chem.* **1949**, *21* (9), 1150−1151.
(96) Capello, C.; Hellweg, S.; Badertscher, B.; Hungerbühler, K. Life-Cycle Inventory of Waste Solvent Distillation: Statistical Analysis of Empirical Data. *Environ. Sci. Technol.* **2005**, *39* (15), 5885−5892.
(97) Underwood, A. J. v. Fractional Distillation of Multicomponent Mixtures. *Ind. Eng. Chem.* **1949**, *41* (12), 2844−2847.
(98) You, J.; Meng, L.; Song, T.-B.; Guo, T.-F.; Yang, Y. M.; Chang, W.-H.; Hong, Z.; Chen, H.; Zhou, H.; Chen, Q.; Liu, Y.; De Marco, N.; Yang, Y. Improved Air Stability of Perovskite Solar Cells via Solution-Processed Metal Oxide Transport Layers. *Nat. Nanotechnol.* **2016**, *11* (1), 75−81.
(99) Leccisi, E.; Fthenakis, V. Life-Cycle Environmental Impacts of Single-Junction and Tandem Perovskite PVs: A Critical Review and Future Perspectives. *Progress in Energy* **2020**, *2*, 032002.
(100) Li, Y.; Meng, L.; Yang, Y.; Xu, G.; Hong, Z.; Chen, Q.; You, J.; Li, G.; Yang, Y.; Li, Y. High-Efficiency Robust Perovskite Solar Cells on Ultrathin Flexible Substrates. *Nat. Commun.* **2016**, *7* (1), 1−10.

https://dx.doi.org/10.1021/acssuschemeng.0c05619
ACS Sustainable Chem. Eng. 2020, 8, 16537−16548